Activity and Stability of a Thermostable α-Amylase Compared to Its Mesophilic Homologue: Mechanisms of Thermal Adaptation†

J. Fitter,*,‡ R. Herrmann,§,|| N. A. Dencher,§ A. Blume,⊥ and T. Hauss#,○

Biologische Strukturforschung, Forschungszentrum Jülich, IBI-2, D-52425 Jülich, Germany, Institut für Biochemie, Technische Hochschule Darmstadt, Petersenstrasse 22, D-64287 Darmstadt, Germany, Institut für Physikalische Chemie, Martin-Luther-Universität Halle-Wittenberg, D-06108 Halle, Germany, Institut für Physikalische Biologie, Heinrich-Heine Universität Düsseldorf, D-40225 Düsseldorf, Germany, and Hahn-Meitner Institut, BENSC, Glienicker Strasse 100, D-14109 Berlin, Germany

Received April 20, 2001; Revised Manuscript Received June 12, 2001

ABSTRACT: To elucidate how enzymes adapt to extreme environmental conditions, a comparative study with a thermostable α-amylase from *Bacillus licheniformis* (BLA) and its mesophilic homologue from *Bacillus amyloliquefaciens* (BAA) was performed. We measured conformational stability, catalytic activity, and conformational fluctuations on the picosecond time scale for both enzymes as a function of temperature. The objective of this study is to analyze how these properties are related to each other. BLA shows its maximal catalytic activity at about 90−95 °C and a strongly reduced activity (only 20% of the maximum) at room temperature. Although *B. licheniformis* itself is a mesophilic organism, BLA shows an activity profile typical for a thermophilic enzyme. In contrast to this, BAA exhibits its maximal activity at about 80 °C but with a level of about 60% activity at room temperature. In both cases the unfolding temperatures T_m are only 6 °C (BAA, T_m = 86 °C) and 10 °C (BLA, T_m = 103 °C), respectively, higher than the temperatures for maximal activity. In contrast to many previous studies on other thermophilic−mesophilic pairs, in this study a higher structural flexibility of the thermostable BLA was measured as compared to the mesophilic BAA. The findings of this study neither indicate a proportionality between the observed dynamics and the catalytic activity nor support the idea of more "rigid" thermostable proteins, as often proposed in the concept of "corresponding states".

A prerequisite for thermophilic organisms to thrive and to survive in extreme environments with temperatures of 70−90 °C and more is a thermal adaptation of their constituents. In particular, the stability and catalytic activity of enzymes are well-known to be highly affected by the temperature. Most proteins from mesophilic organisms are not able to resist high temperatures, because they lose their specific three-dimensional structure by thermal unfolding or suffer from thermoinactivation due to other mechanisms such as deamidation of Asn/Gln residues (*1*, *2*). Therefore, thermal adaptation of thermophilic enzymes is characterized by proteins (i) keeping their folded and native structure at high temperatures and (ii) showing sufficient catalytic activity under the same conditions. These remarkable properties of thermozymes have attracted increasing attention, because they are important for many biotechnological applications (*3*). The comparison of homologous enzymes with different thermostabilities offers a unique opportunity to elucidate strategies for thermal adaptation. Despite their enormously different thermostabilities, thermophilic enzymes and their mesophilic counterparts often share the same catalytic mechanism, a high sequence homology, and a rather similar three-dimensional structure (*4*−*6*). Many experimental approaches have been applied to identify determinants of thermostability. Thermostability in different thermozymes seems not to be achieved by a general universal strategy but by a combination of individual strategies, such as an increased number of hydrogen bonds and salt bridges, an optimized packing of the hydrophobic core, shortened surface loops, increased number of prolines, and an increase in buried hydrophobic residues (*3*, *7*, *8*). It is a widely assumed view that most of the these stabilizing determinants are associated with a decrease of structural flexibility (*3*, *9*). Surprisingly, several recent studies comparing mesophilic and thermophilic proteins did not support this hypothesis (*10*−*13*). Nevertheless, conformational flexibility not only is a parameter that has an impact on protein stability but is, on the other hand, significant for catalytic activity. Therefore, a reasonable balance between rigidity and flexibility of the protein structure, well tuned with respect to the environmental conditions (elevated temperatures), which strongly influence dynamical properties, is one of the key elements for thermal adaptation.

In this paper, we address the question of how thermal adaptation is achieved in the case of α-amylase. In particular, we are interested in how stability, catalytic activity, and

† This work was supported by Grant 03-DE5DA1-8 from Bundesministerium für Forschung und Technologie and by Fonds der Chemischen Industrie.

* Corresponding author. Phone: +49 2461 612036. Fax: +49 2461 612020. E-mail: j.fitter@fz-juelich.de.

‡ Forschungszentrum Jülich.

§ Technische Hochschule Darmstadt.

|| Present address: Charité, Institut für medizinische Physik und Biophysik, Humboldt-Universität, D-10098 Berlin, Germany.

⊥ Martin-Luther-Universität Halle-Wittenberg.

Heinrich-Heine Universität Düsseldorf.

○ Hahn-Meitner Institut.

10.1021/bi010808b CCC: $20.00 © 2001 American Chemical Society
Published on Web 08/09/2001

conformational flexibility are related. For this purpose we studied two α-amylases, both from mesophilic sources, but with very different thermostabilities. Supplementary to a mesophilic α-amylase from *Bacillus amyloliquefaciens* (BAA)[1] we analyzed an extreme thermostable α-amylase from *Bacillus licheniformis* (BLA) which is widely used in industrial processes of starch degradation (*14*). Although *B. licheniformis* itself is an mesophilic organism, it produces a very heat-resistant α-amylase[2] that is even more thermostable than the related enzyme produced by thermophilic organisms, such as *Bacillus stearothermophilis* (*15*). To characterize the structural stability of both enzymes, we determined stability curves by measuring tryptophan fluorescence as a function of temperature. These stability studies were supplemented by measurements using DSC. The catalytic enzyme activity was determined with the natural substrate (starch) in the same temperature range. In addition, neutron spectroscopy was applied to monitor fast structural fluctuations in both enzymes occurring on the picosecond time scale. These essential thermal equilibrium fluctuations as well as their temperature dependence directly reflect the response of the protein structure to a particular environmental condition or a change in these conditions. There is much evidence that nature has optimized not only structural features but also dynamical properties of these structures to provide molecules most efficiently adapted to their biological function (see, for example, refs *16*−*18*).

EXPERIMENTAL PROCEDURES

Enzymes. α-Amylase is an amylolytic enzyme that hydrolyzes starch, glycogen, and related polysaccharides by cleaving internal α-1,4-glycosidic bonds (*14*). For all comparative studies α-amylase from *B. licheniformis* (BLA, thermophilic enzyme, 58 550 Da; purchased from Sigma-Aldrich) and from *B. amyloliquefaciens* (BAA, mesophilic enzyme, 58 403 Da; purchased from Fluka) were used. SDS−polyacrylamide gel electrophoresis revealed single bands for each enzyme, indicating purity for α-amylase material as obtained from the producers. Although only the three-dimensional structure of BLA has been determined so far [see Figure 1 (*19*)], there is much evidence that the structure of BAA is very similar. Both enzymes consist of a monomer with three domains exhibiting an (β/α)-barrel as a central structure unit. Sequence alignment of BLA and BAA revealed a very high homology (81% identity, 88% similarity; see ref *19*). The enzymes were dissolved in buffer with 30 mM Mops and 50 mM NaCl at pH 7.4. Due to three calcium binding sites in both structures of α-amylase, the calcium concentration plays an essential role for thermostability (*20*−*22*). In α-amylase as purchased from the distributor the calcium binding sites are not fully saturated. Therefore, to obtain defined and reproducible conditions, 1 mM $CaCl_2$ was added to the buffer for saturating all calcium binding sites and 1 mM $CaCl_2$ plus 20 mM EDTA was added to obtain calcium-free α-amylase.

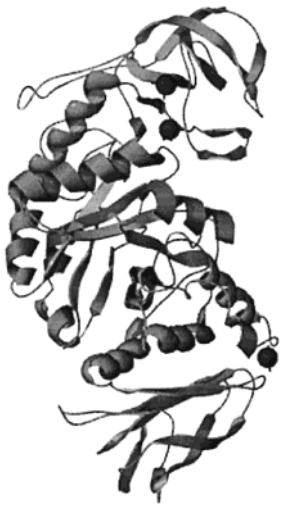

FIGURE 1: Crystal structure of α-amylase from *B. licheniformis* (BLA; PDB entry 1BLI). The structure is characterized by three distinct domains, a central (β/α)-barrel (domain A), domain B (upper part of the structure) and domain C (lower part). The positions of calcium binding sites (solid circles) indicate the importance of calcium for stabilizing the structure by forming additional links connecting domains C and A as well as domains B and A. The substrate binding site is localized in a cleft between the central domain A and domain B.

Fluorescence Spectroscopy. Protein unfolding was monitored by measuring the fluorescence from aromatic residues (phenylalanine, tyrosine, tryptophan), where contributions from Trp residues dominate the fluorescence emission near 340 nm (for more details, see refs *23* and *24*). Protein solutions (enzyme concentrations, 0.01 mg/mL) were filled into quartz cuvettes with a light path length of 1 cm. Fluorescence emission changes for both α-amylases (each with 17 Trp residues per molecule) were monitored with the Luminescence Spectrometer LS 50B (Perkin-Elmer) as a function of temperature, applying excitation and emission wavelengths of 280 and 342 nm, respectively. For these measurements heating rates between 0.2 and 1 °C/min were used. The intensities obtained were corrected for intrinsic temperature dependence of tryptophan fluorescence as described elsewhere (*25*). In addition, measurements as a function of GdmCl concentration and of pH were performed in order to monitor chemical unfolding transitions.

Differential Scanning Calorimetry. To study thermal unfolding at temperatures near and above 100 °C, calorimetric measurements were performed using a VP-DSC MicroCalorimeter (MicroCal). To avoid evaporation of aqueous solutions at high temperatures, excess pressure (2 bars) was applied. Measurements were carried out by applying a heating rate of 1 °C/min and with enzyme concentrations of 0.09 mg/mL in 0.5 mL solution volume. Thermograms with subtracted baselines were analyzed and fitted to determine T_m and ΔH_m using the MicroCal Origin software.

Enzyme Activity. For enzymatic activity measurements as a function of temperature the starch−iodine method was used (*26*, *27*). This method is well suited for temperature-dependent measurements, because activities are measured effectively at the chosen incubation temperatures between

[1] Abbreviations: BLA, *Bacillus licheniformis* α-amylase; BAA, *Bacillus amyloliquefaciens* α-amylase; DSC, differential scanning calorimetry; T_m, melting temperature; ΔH_m, enthalpy change upon thermal unfolding; ΔS_m, entropy change; ΔG_{unf}, Gibbs free energy change; ΔC_p, change in heat capacity; Mops, 3-(*N*-morpholino)-propanesulfonic acid; EDTA, ethylenediaminetetraacetic acid; GdmCl, guanidinium chloride; E_a, activation energy for enzyme catalysis; T_{opt}, temperature of maximum catalytic activity; INS, incoherent neutron scattering.

[2] For simplicity we denote BLA as a thermophilic enzyme.

20 and 100 °C. Five milliliters of substrate solution (10 mg/mL starch from corn dissolved in standard buffer, 30 mM Mops, 50 mM NaCl, 1 mM $CaCl_2$, pH 7.4) was added in a test tube and maintained for 10 min at an incubation temperature. An enzyme solution (0.025 mg/mL) with standard buffer was prepared and warmed to the same temperature. Subsequently, 0.5 mL of enzyme solution was added to the substrate solution, keeping this during 5 min reaction time at the incubation temperature. The digest is then added to 5 mL of stopping reagent (0.1 M HCl) at room temperature. After mixing, 0.5 mL of this mixture was added to 5 mL of iodine−iodide solution (0.05 mg/mL iodine and 0.5 mg/mL potassium−iodine in H_2O). The intensity of the blue color (absorbance at 620 nm), which is characteristic for the substrate−iodine complex, was measured in a spectrometer (UV-2101PC, Shimadzu). The enzyme activity was calculated by using

$$\text{activity (unit/mL)} = D[(R_0 - R)/R_0] \times 100 \qquad (1)$$

where R_0 is the absorbance of the substrate−iodine complex in the absence of enzyme, R is the absorbance of the digest, and D is the dilution factor of the enzyme.

Neutron Spectroscopy. For both enzymes an amount of 125 mg of α-amylase was dissolved in 2.5 mL of D_2O buffer (standard buffer conditions; see Enzyme Activity) and filled into a slab-shaped aluminum sample container [inner sample volume: 40 mm (width) × 50 mm (height) × 1 mm (thickness)], which was closed with a cap using a Teflon ring sealing. Neutron scattering experiments have been carried out using the time-of-flight (TOF) spectrometer NEAT (Hahn-Meitner Institut, Berlin) (*28*, *29*). TOF spectra were measured using an incident wavelength of 5.1 Å, with an elastic energy resolution of 94 μeV, and within an angular range of $13.3° \leq \phi \leq 136.7°$. The required sample temperatures were set using a cryofurnace. All samples, including the vanadium standard, pure buffer solution, and the empty can, were measured with a sample orientation angle of $\alpha = 135°$ with respect to the incident neutron beam direction. The TOF spectra were corrected, normalized, grouped, and transformed to the energy transfer scale. For our purpose a measuring time of about 7 h at NEAT was adequate for sufficient counting statistics. Due to strong solvent scattering, spectra from pure buffer were subtracted from spectra of enzyme solutions. The difference spectra obtained represent scattering mainly related to incoherent scattering from nonexchangeable H-atoms of α-amylase (about 3400 per α-amylase molecule). In a neutron scattering experiment with predominantly incoherent scattering the double differential cross section

$$\frac{\delta^2\sigma}{\delta\Omega\delta\omega} = \frac{1}{4\pi}\frac{|\mathbf{k}_1|}{|\mathbf{k}_0|}[{b_{\text{inc}}}^2 S_{\text{inc}}(\mathbf{Q},\omega)] \qquad (2)$$

determines the number of neutrons scattered into a solid angle element $\delta\Omega$ and an energy transfer element $\delta\omega$. Here b_{inc} denotes the incoherent scattering length, while $\mathbf{k_0}$ and $\mathbf{k_1}$ are the wave vectors for the incident and scattered neutrons, respectively (with momentum transfer $\mathbf{Q} = \mathbf{k_1} - \mathbf{k_0}$). The spectra obtained, which were grouped from originally 140 spectra into 11 spectra, were fitted using

$$S_{\text{inc}}(Q,\omega) = F e^{-\hbar\omega/(2k_BT)}[S_{\text{theor}}(Q,\omega) \otimes S_{\text{res}}(Q,\omega)] + B \qquad (3)$$

applying a convolution (⊗, energy convolution operator) with the resolution function $S_{\text{res}}(Q,\omega)$ (obtained from vanadium measurements). F denotes a normalization factor and $\exp(-\hbar\omega/2k_BT)$ gives the detailed balance factor. B is a constant background. Considering the diffusive character of equilibrium fluctuations occurring in the enzyme, the quasi-elastic broadening observed in the spectra was fitted by Lorentzians. Therefore, the theoretical scattering function

$$S_{\text{theor}}(Q,\omega) = e^{-\langle u^2\rangle Q^2}[A_0(Q)\delta(\omega) + A_1(Q)L_1(H_1,\omega)] \qquad (4)$$

is parametrized by the elastic and quasi-elastic incoherent structure factors A_0 and A_1, respectively, and the width of the quasi-elastic contribution $H_1 = (\tau_1)^{-1}$. The scattered intensity is separated into an elastic $\delta(\omega)$-shaped component (experimentally observed with the resolution width Γ_{res}) and a quasi-elastic Lorentzian-shaped contribution $L_1(H_1,\omega)$ (see Results, Figure 7). The data analysis applied allows to study fluctuations with correlation times of approximately 0.1−10 ps and with amplitudes ranging from 0.5 to 4 Å. For further methodical details, see refs *17* and *30*.

RESULTS

Conformational Stability. Gibbs free energy of the unfolding transition is determined by enthalpic ΔH and entropic ΔS contributions

$$\Delta G_{\text{unf}}(T) = G^{\text{U}} - G^{\text{F}} = \Delta H(T) - T\Delta S(T) \qquad (5)$$

In a reversible two-state unfolding process $\Delta G_{\text{unf}}(T)$ describes the ratio between molecules in the ensemble being in the folded state as compared to those in unfolded state at the given temperature. A positive value of ΔG_{unf} corresponds to an ensemble with the major proportion of proteins in the folded state (for more details, see ref *31*). At the melting temperature T_m with $\Delta G_{\text{unf}}(T_m) = 0$, where enthalpic and entropic contributions compensate each other, an equilibrium between proteins in the folded and unfolded state is achieved in the ensemble. Although both α-amylases we study here do not unfold reversible in a typical two-state process (*15*, *22*, *32*), T_m values can be obtained from sigmoidal stability curves as shown in Figure 2. Both α-amylases show a pronounced dependence of T_m on the calcium concentration (see Table 1). The distinct effect of calcium for stabilizing both protein structures is indicated by an enormous increase of the melting temperatures by more than 40 °C due to calcium saturation. At least for BLA the calcium effect is not surprising, because the calcium binding sites are located at strategic positions in the structure providing additional stabilizing connections between the three domains (see Figure 1). The high sequence homology between BLA and BAA and the fact that the residues involved in calcium binding are mainly conserved in the BAA structure indicate large similarities in calcium binding for both enzymes (see refs *19* and *21*). The measurements have been performed with different heating rates. In particular, for calcium-free samples (i.e., with EDTA) the heating rate has a strong influence on the corresponding melting temperatures. Heating rates of 0.2

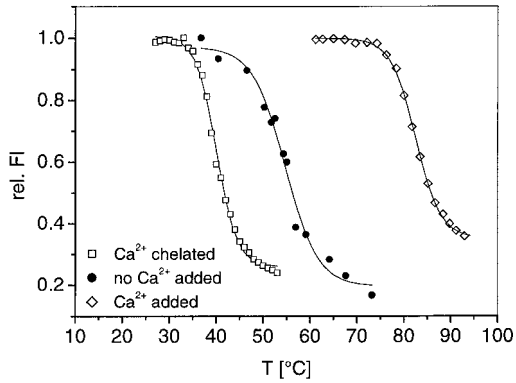

FIGURE 2: Stability curves of α-amylase as determined by tryptophan fluorescence emission intensities. All curves (here only for BAA), measured with enzymes in buffer with different calcium concentration, show a sigmoidal shape representing thermal unfolding transition. The midpoint of these transition curves denotes the melting temperature T_m. An increase in calcium concentration shifts T_m to higher temperatures [Ca^{2+} chelated, 20 mM EDTA added to the standard buffer; heating rate, 0.2 °C/min; no Ca^{2+} added, a low (a few micromolar) but unknown amount of Ca^{2+}; heating rate, 0.5 °C/min; Ca^{2+} added, standard buffer with 1 mM $CaCl_2$; heating rate, 1 °C/min]. The corresponding melting temperatures T_m from measurements with BAA and BLA are given in Table 1.

Table 1: Thermodynamic Parameters of α-Amylase Thermal Unfolding[a]

	BAA			BLA		
	T_m (°C)	ΔH_m (kJ mol^{-1})	ΔS_m (kJ mol^{-1} K^{-1})	T_m (°C)	ΔH_m (kJ mol^{-1})	ΔS_m (kJ mol^{-1} K^{-1})
with EDTA	40			52		
without $CaCl_2$/EDTA	54			76		
with $CaCl_2$	86	1412	3.93	103	1521	4.04

[a] Thermodymamic parameters as obtained from fluorescence spectroscopy and from DSC. The parameters for the most stabilizing conditions (with $CaCl_2$) were determined by DSC (see Figure 3). Enthalpy and entropy changes have been calculated from DSC data.

°C/min and less gave T_m values of about 40 °C for BAA and 52 °C for BLA. With larger heating rates of 1 °C/min we observed for these calcium-free samples T_m values of 53 °C (BAA) and 62 °C (BLA) (data not shown). These results indicate that in the case of heating rates above 0.2 °C/min an equilibrium at the given temperature is not reached. This behavior is caused by an irreversible step in the denaturation process (see Discussion). For other buffer conditions (i.e., no Ca^{2+} added and Ca^{2+} added) we do not observe this strong dependence on the heating rate. In particular, for Ca^{2+}-saturated α-amylase (with 1 mM $CaCl_2$) the T_m value is shifted only by about 1 °C, if changing the heating rate from 0.2 to 1 °C/min.

Besides the strong calcium effect, there is still an intrinsic higher conformational stability for the thermophilic BLA as compared to the mesophilic BAA. For all conditions BLA shows T_m values larger by 12−22 °C as compared to those from BAA. This difference in the conformational stability between both enzymes is supported by measurements of the unfolding transition caused by chemical denaturants (see Figure 3A). BLA in the calcium-free state needs a higher concentration of GdmCl to unfold than BAA. The absolute values of $[GdmCl]_{1/2}$ are rather small for both α-amylases, because the enzymes are already destabilized by calcium

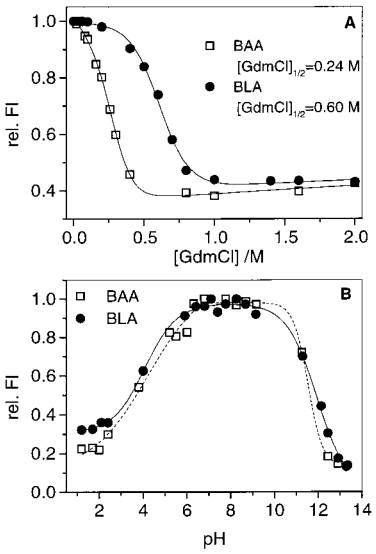

FIGURE 3: (A) Stability curves measured at room temperature (23 °C) as a function of the chemical denaturant GdmCl. Both enzymes were measured in buffer with 20 mM EDTA corresponding to calcium-free α-amylase. $[GdmCl]_{1/2}$ denotes the concentration of GdmCl which corresponds to the equilibrium in the ensemble between the folded and the unfolded state (it is the equivalent to T_m in the thermal unfolding). (B) Stability curves measured at 40 °C as a function of pH. Unfolding in the region of acidic low pH (<6.0) and in basic high pH (>9.0) was described with sigmodial curves (BLA, dashed lines; BAA, solid lines). The corresponding midpoints are rather similar for both enzymes (BAA, $pH_{1/2}$ 4.0 and 11.5; BLA, $pH_{1/2}$ 4.1 and 11.9).

extraction (see Table 1). In contrast to the difference in chemical denaturation caused by GdmCl, the pH dependence of stability is rather similar for both enzymes (Figure 3B). For BLA as well as for BAA the native structure is stable between 6.0 < pH < 9.0. The destabilizing effect occurring at extreme pH values is caused by repulsive electrostatic energies between charged groups and by energy changes associated with the burial of ionized groups (see, for example, ref *33*). As shown in the thermograms of Figure 4, the unfolding of BLA and BAA is not characterized by a sharp cooperative transition as often found for pure two-state unfolding processes of smaller single-domain proteins (*34*). Nevertheless, the unfolding of both enzymes occurs "quasi-cooperatively" since the three individual transitions contributing to the single peak in the thermogram have T_m values rather close to each other. For both enzymes a number of three transitions fits the data most reasonable. Furthermore, the "width" of the transition spans in both cases approximately 20 °C. Besides the fact that both transitions are separated on the temperature scale by 17 °C, the thermal unfolding process is qualitatively rather similar for both enzymes. For both enzymes, contributions from protein association/dissociation to the transition peaks can be ruled out, because the T_m values did not show any dependence on enzyme concentrations (data not shown). The fact that a number of three separated subtransitions occur during the thermal unfolding suggests a relation to the three-domain structure of α-amylase. Recently, Feller et al. (*22*) observed a rather similar thermal unfolding for BLA and BAA with three individual transitions. Furthermore, also for α-amylase from the thermophilic *Pyrococcus furiosus* the thermal unfolding was best described by three separate subtransitions (*35*). Alternatively to the assumption that each subtransition

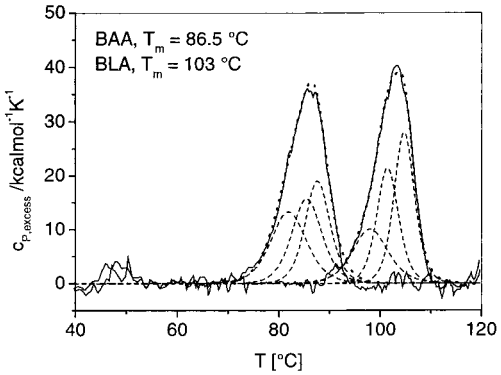

FIGURE 4: Thermograms measured with both enzymes in standard buffer (i.e., saturated calcium binding sites) using DSC. For both enzymes the peak in heat capacity change as a function of temperature, specifying the thermal unfolding transition, can be deconvoluted into three nearly cooperative transitions, represented by Gaussian curves (dashed lines). The sum of the Gaussians (dotted lines) fit the experimental values (solid lines). These transitions revealed individual T_m values rather close to each other (BAA, T_{m1} = 82 °C, T_{m2} = 85.5 °C, T_{m3} = 87.6 °C, mean T_m = 86.5 °C; BLA, T_{m1} = 97 °C, T_{m2} = 102 °C, T_{m3} = 105 °C, mean T_m = 103 °C). The integrated peak intensity (sum of the Gaussians) gives the enthalpy change during thermal unfolding ΔH_m.

reflects the unfolding of an individual domain, a "hierarchic running unfolding process" is more probable. In the latter case, a higher thermal-induced mobility of domains C and B with respect to the central domain A might be related to the first subtransition, before subsequent transition domain unfolding occurs. As shown in Figure 1 the compactness of the α-amylase structure and the relative mobility of domains B and C with respect to domain A are strongly determined by the calcium. Supporting this view, DSC thermograms from calcium-free α-amylase (data not shown) revealed much broader "peak structures" (with clearly separated peaks) which are shifted to lower temperatures.

Temperature Dependence of Catalytic Activity. Enzyme activities were determined using the starch−iodine method in a temperature range between 20 and 100 °C (Figure 5). In this temperature range the substrate (starch) is stable and senses no modifications which might affect the determination of enzyme activity (see Experimental Procedures). As shown in Figure 5A the catalytic activity differs significantly in the low-temperature region between both enzymes. Surprisingly, the thermostable BLA shows a behavior, typical for a real thermophilic enzyme, despite the fact that BLA originates from a mesophilic source. The activity for BLA at moderate temperatures (20−40 °C) is only 20−40% of the maximum activity reached at a temperature of about 90 °C (T_{opt}). Even above 90 °C up to 100 °C the activity for BLA is near the maximum value. In contrast to this, the mesophilic BAA exhibits already in the low-temperature region an activity which more than 60% of the maximum value, which is reached at 80 °C (T_{opt}). Above this temperature BAA is irreversibly inactivated. The low catalytic activity of BLA at moderate temperatures is related to high catalytic activation energies as given in Figure 5B. In particular, in the temperature region between 25 and 40 °C E_a from BLA is more than 6 times larger as compare to the corresponding value obtained for BAA. At temperatures above 50 °C the activation energy of BLA is only larger by a factor of 1.5 than that of BAA. Despite these significant differences in the temperature dependence of the enzyme activity, the

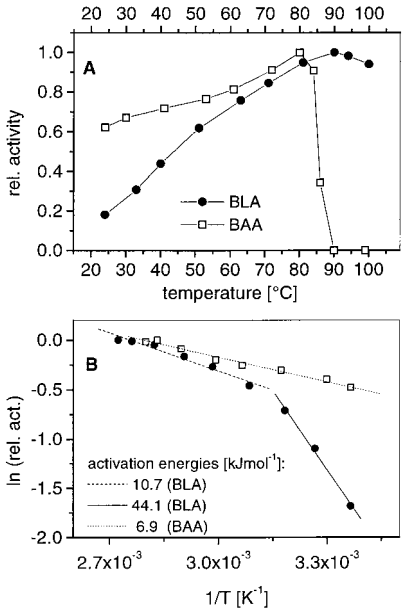

FIGURE 5: α-Amylase activity as function of temperature. (A) The relative catalytic activities are shown as determined for α-amylase in standard buffer (under calcium saturation). The absolute activities of both enzymes at their individual optimal temperatures (BAA, T_{opt} = 80 °C; BLA, T_{opt} = 90 °C) are the same within the limit of error (approximately ±5%). (B) Arrhenius plot of the data shown above in order to determine activation energies for the catalytic process. While only one activation energy (6.9 kJ mol^{-1}) describes the temperature dependence of BAA within a temperature range from 25 to 80 °C, a fit with two activation energies (25−40 °C, E_a = 44.1 kJ mol^{-1}, and 50−90 °C, E_a = 10.7 kJ mol^{-1}) is necessary to represent the temperature dependence of BLA.

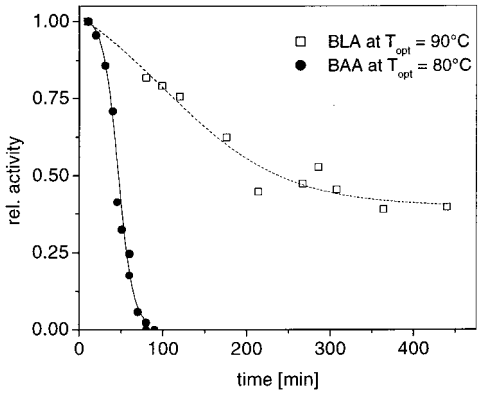

FIGURE 6: Relative enzymatic activities as a function of time for both enzymes in standard buffer incubated at their individual optimal temperatures T_{opt}.

mechanism of thermal inactivation seems to be qualitatively rather similar for both α-amylases: in both cases the maximum activity is reached at a temperature (T_{opt}) just a few degrees below the individual melting temperature. Besides the question at which temperature an enzyme shows a maximal activity, it is important to know how long this high level of activity can continue at that temperature. In particular, for industrial starch processing α-amylase must keep its activity at high temperatures for a time as long as possible. Figure 6 demonstrates why BLA is so widely used for industrial applications. After a more pronounced initial decrease in activity, it keeps a rather high level of activity for several hours at T_{opt}, while BAA loses its activity at the corresponding T_{opt} within a much shorter time. The data present here have been obtained from measurements with

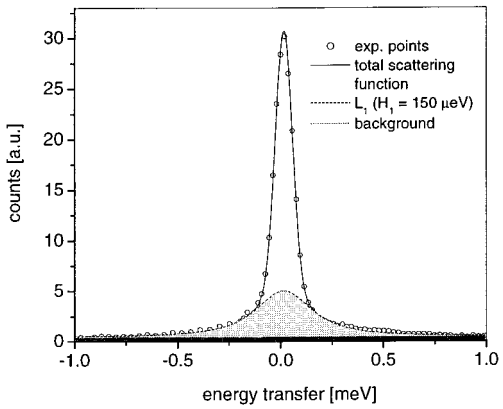

FIGURE 7: Energy transfer spectrum representing incoherent neutron scattering of nonexchangeable hydrogen atoms in α-amylase solution. To determine the amplitude of quasielastic scattering A_1 (represented by the light gray area under the Lorentzian L_1 which is related to structural fluctuations), the experimental spectrum (circles) is fitted by expressions given in Experimental Procedures (eqs 3 and 4).

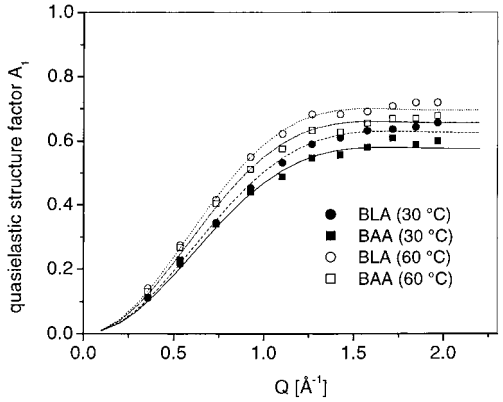

FIGURE 8: Quasi-elastic structure factors representing structural fluctuations on the picosecond time scale. The given values (symbols) were obtained from analysis of the experimental data (see Figure 7). Further analysis by fitting the data with simple analytical models (lines) is described elsewhere (*37*).

α-amylase under calcium saturation. Other measurements (not shown here) with calcium-free amylase at room temperature revealed that calcium has no effect on the catalytic activity. In contrast to this, lower activity values were observed with increasing temperature as compared to calcium-bound α-amylase. This indicates that calcium has not a direct impact for the catalytic mechanisms but preserves enzymatic activity at higher temperatures due to the stabilizing effect. This behavior was observed for both α-amylases, BLA and BAA.

Conformational Flexibility. Incoherent neutron scattering (INS), which is a commonly used technique in neutron spectroscopy, makes use of a large incoherent cross section of hydrogen nuclei (∼ 40 times larger than incoherent cross sections of other elements in biological samples) and is well suited to study internal molecular motions in a time range from 10^{-9} to 10^{-14} s. Using the enzymes dissolved in D_2O, all nonexchangeable hydrogens (which are distributed "quasi-homogeneously" in the molecule) serve as probes to monitor local fluctuations occurring in the structure. In a neutron scattering experiment with predominantly incoherent scattering, information on the dynamics of individual hydrogen atoms can be obtained from the incoherent scattering function $S_{inc}(Q,\omega)$ using the formalism of self-correlation functions (see, for example, ref *36*). According to the diffusive and liquidlike character of the predominant part of the motions (with samples at physiological conditions), the quasi-elastic scattering is in the focus of our analysis (see Figure 7). Figure 8 shows the Q dependence of the quasi-elastic structure factors (A_1 values) as measured at 30 °C (solid symbols) and at 60 °C (open symbols). The Q dependence of A_1 looks qualitatively rather similar for all measurements. Because we observe localized fluctuations, mainly reorientational movements of polypeptide side groups, A_1 starts at zero in the low Q range (Q is related to an inverse amplitude). An increase of A_1 with increasing Q (i.e., the slope of A_1 in Q) for the data shown here is related to motions with amplitudes in the range between 2 and 3 Å in average. Above $Q = 1.5$ Å^{-1} a constant level with A_1 values between 0.6 and 0.7 is reached. These values give the fraction of hydrogens (normalized to the unity) in the protein structure participating in motions visible in our Q-ω window. This fraction of hydrogens performing the observable motions and the amplitudes of these motion are directly reflecting the conformational flexibility of the systems. As expected, the data from measurements performed at 60 °C show larger A_1 values and therefore a higher conformational flexibility as compared to the 30 °C data. Interestingly, for both temperatures the thermophilic BLA shows larger A_1 values compared to BAA, indicating a higher conformational flexibility for BLA. Within the limits of error, these differences (high Q A_1 values approximately 6−7% larger for BLA) are the same for both temperatures. Although theses differences are small, they are significant and fully reproducible [as shown in earlier experiments (*12*)]. A more detailed analysis using simple analytical models to interpret the experimental data is described elsewhere (*37*).

DISCUSSION

Because of its biotechnological potential the mechanisms and determinants of α-amylase thermostability (in particular for BLA) have already been studied in the past (*15*, *21*, *32*, *35*) and are still in the focus of actual research (*38*−*40*). The fact that BLA as well as BAA exhibits irreversible denaturation was already observed by Tomazic and Klibanov (*15*). Therefore, they proposed a simple scheme which involves one step of reversible unfolding and a subsequent step of irreversible inactivation (*41*):

$$N \overset{K_{unf}}{\leftrightarrow} U \overset{K_{in}}{\longrightarrow} I \qquad (6)$$

where N is the native fully active state, U is the thermally unfolded state, and I is the irreversibly inactivated state. Information about the first transition can be obtained from data characterizing the conformational unfolding, while parameters describing the second transition can be extracted from temperature-dependent activity measurements. Both kinds of measurements have been performed in the present study. By comparing melting temperatures (Table 1) and the corresponding temperatures of maximal catalytic activity (T_{opt}; see Figure 5A), we find T_{opt} values which are 6−13 °C below the melting temperatures. Although not visible in our data, BLA also shows a drastic irreversible inactivation, similar to that of BAA, but at temperatures above 105 °C (*21*). T_m values and T_{opt} values are shifted similarly to higher

temperatures for BLA as compared to BAA, and the difference between T_{opt} and T_m is, within the limits of error, rather similar (10 °C in average) for both enzymes. These observations support the fact that the irreversible process is rather similar in both enzymes while the reversible thermal unfolding is different for BAA and BLA (BAA, $T_m = 86.5$ °C; BLA, $T_m = 103$ °C). A similar hypothesis, based on thermoinactivation studies only, was proposed by Tomazic and Klibanov (*15*).

The question which structural features are responsible for the higher thermostability of BLA with respect to BAA is still not fully clarified yet. Unfortunately, only the BLA structure has been solved, and therefore a comparison at the level of an atomic model is not possible. From studies on BLA it is supposed that mainly two features contribute to BLA thermostability: (i) the region between domain A and domain B stabilized by the triadic Ca−Na−Ca metal binding site which is surrounded by a network of electrostatic interactions and (ii) some additional salt bridges in other regions of the structure (*21*, *38*). By comparing the difference in melting temperatures between calcium-free and calcium-saturated α-amylases, we find a little more pronounced "calcium-induced" conformational stabilizing in BLA (52 vs 103 °C; $\Delta T_m = 51$ °C) as compared to BAA (40 vs 86 °C; $\Delta T_m = 46$ °C). A more pronounced difference of stabilization between BLA and BAA is found for other contributions not related to calcium (BAA, $T_m = 40$ °C, vs BLA, $T_m = 52$ °C). The different susceptibilities to chemical denaturants, as shown in Figure 3A, confirm the importance of further stabilization mechanisms not related to calcium binding.

The hypothesis that stabilization features, like additional salt bridges, make the protein structure less flexible and therefore more stable is only one part of the story. Conformational motions which are part of motions in the unfolding pathway can be hindered by additional hydrogen bonds or salt bridges and stabilize the structure. Certainly, the reduction of these motions leads to a reduced flexibility (i) in the corresponding region of the protein and (ii) with respect to the particular time scale of these motions. At the same time additional conformational motions occurring in other regions of the proteins structure and /or at different time scales can stabilize the folded state. If these motions increase the conformational entropy of the folded state with respect to the unfolded state, a resulting change of conformational entropy during unfolding ΔS_{unf} will be smaller, and increased flexibility (of the folded state) has a stabilizing effect (see eq 5). Therefore, the larger conformational flexibility on the picosecond time scale observed for BLA as compared to BAA is not contradictory to their corresponding thermostabilities (see Figure 8). In fact, these results and further studies on the dynamical behavior of α-amylases in the unfolded state indicate that mechanisms of entropic stabilization contribute to the high thermostability of BLA (*12*, *37*). Such a mechanism to achieve thermostability was also proposed for other proteins (*42*, *43*) and is in some cases supported by a higher conformational flexibility of the more thermostable protein (*44*). On the other hand, most studies published so far indicate a reduced conformational flexibility for the thermophilic enzyme as compared to the mesophilic homologue (*4*, 5, *8*, *45*−*50)*. These opposed findings indicate that an universal mechanism for thermostabilization seems not to be present in nature. Interestingly, in a study which compares structural features of thermohilic and mesophilic (β/α)-barrel hydrolases (including α-amylases), in average, higher crystallographic thermal *B*-factors were observed for the thermophilic enzymes (*13*). Although crystallographic *B*-factors have to be considered with caution because they often include other contributions which are not related to dynamical properties of the proteins, these results support our finding of a thermostable α-amylase, which is characterized by a higher conformational flexibility as compared to their mesophilic counterparts. A meaningful parameter for analyzing mechanisms of thermostability is given by Gibbs free energy ΔG as a function of temperature (see eq 5). For many proteins (and for the first process N ↔ U in our case) ΔG as a function of temperature can be described by a parabolic bell-shaped curve intersecting the abscissa (i.e., $\Delta G = 0$) twice, indicating a "cold denaturation" in the low-temperature region and a thermal unfolding at T_m at high temperatures (*30*). It is obvious from these stability curves that a high thermodynamic stability (i.e., ΔG_{max}, often found at room temperatures) is not necessarily related to a high thermal stability (i.e., large T_m). Therefore, the analysis of structural properties, supposed to be important for protein stability, can give only a limited amount of information about mechanisms of thermal adaptation.

Among possible effects of conformational flexibility on protein stability the fluctuations, observed in this study, may also be correlated to catalytic properties. Equilibrium fluctuations on the picosecond time scale are supposed the be required for catalytic activity, because they help to overcome barriers in the conformational energy landscape of the proteins and thereby "lubricate" conformational changes on longer time scales (micro- to milliseconds) which are often directly related to the catalytic mechanism (see, for example, refs *16* and *17*). With respect to the mesophilic BAA, larger catalytic activation energies for BLA (Figure 5A) are found for the same temperature range ($T < 60$ °C), where picosecond fluctuations in the BLA structure are more pronounced as compared to BAA (Figure 8). This result is somehow surprising and offers many possible explanations. Maybe the active site (substrate binding site) is more rigid in BLA and exhibits higher energy barriers as compared to BAA. In this case even more pronounced (overall) conformational fluctuations in BLA would not be sufficient to overcome these particular energy barriers at lower temperatures. Another interesting feature in this respect is the fact that catalytic activity and conformational flexibility, as observed here, are not proportional. A much larger difference in activity between both enzymes is observed for 30 °C as compared to 60 °C, while for both temperatures the difference in flexibility is rather similar. Although the correlation of catalytic and dynamic properties has already been analyzed in detail for various proteins (*51*−*53*), a comparison of these properties between *different* proteins is not straightforward. In particular in our case, where (i) detailed structural information is available only for BLA and (ii) obtained dynamical properties are averaged over the whole structure (i.e., without spatial resolution), an interpretation of how these two properties are related can only be rather speculative. On the basis of the results presented here, we can, nevertheless, state that aspects of the "corresponding states" hypothesis are not confirmed by our example of mesophilic

and thermophilic α-amylase. This widely accepted view concerning the relation between mesophilic and thermophilic proteins proposes that the enzymes show a conformational flexibility and, directly related to this, a catalytic activity which is more or less the same at their individual (physiological) temperatures (*8*, *9*, *45*, *47*). This direct proportionality between activity and flexibility, observed for example in studies where H/D-exchange kinetics were measured to obtain information about enzyme flexibility (*47*), was not found for the α-amylase pair (see also ref *12*). It is obvious that deviations from this strict flexibility−activity relation can occur when a broader spectrum of time scales for conformational fluctuations is involved and when part of these fluctuations contribute to effects, such as entropic stabilization. A remarkable feature in the temperature dependence of the catalytic activity (Figure 5A) is the fact that both enzymes need very high temperatures (just a few degrees below T_m) to achieve maximal activity. Maybe the vicinity of the substrate binding site to the Ca−Na−Ca metal binding site, which is important for protein stability (see above), makes the active site rather "rigid" and allows maximal activity only at rather high temperatures. Due to this coupling the more pronounced calcium-effected stabilization in BLA as compared BAA may correspond to the lower catalytic activity of BLA at lower temperatures. Similar observations have already been made for various other proteins, where, for a high thermal stability, an enzyme must "pay the price" of a loss in catalytic efficiency (*46*, *54*). In this context it is important to note that BLA shows this loss in activity only in the low-temperature region. At high temperatures (80 °C for BAA and 90 °C for BLA) the absolute catalytic activity is nearly the same for both enzymes.

As pointed out in this study, one key to elucidate the interplay of activity and stability in enzymes is a really detailed knowledge of conformational fluctuations occurring in the structures. Although often difficult to obtain, we need to know the dynamic properties on a *broad spectrum of time scales* and with *spatial resolution*. In particular, this kind of information will give us the chance to decide whether particular structural fluctuations are related to functional properties and/or have an impact on the stability. Only on the basis of this knowledge will we be able to figure out which properties are varied by nature to adopt enzymes to extreme environmental conditions.

ACKNOWLEDGMENT

We thank R. E. Lechner and the Hahn-Meitner-Institut (Berlin) for help during neutron scattering experiments and for providing neutron beam facilities. Furthermore, we are indebted to Mrs. Fölting (Universität Halle) for support with DSC measurements. J.F. thanks G. Büldt (Forschungszentrum Jülich) for many stimulating discussions and for continuous support in his Institute.

REFERENCES

1. Tanford, C. (1970) *Adv. Protein Chem. 24*, 1−95.
2. Zale, S. E., and Klibanov, A. M. (1986) *Biochemistry 25*, 5432−5444.
3. Vielle, C., and Zeikus, J. G. (1996) *Trends Biotechnol. 14*, 183−190.
4. Wallon, G., Kryger, G., Lovett, S. T., Oshima, T., Ringe, D., and Petsko, G. A. (1997) *J. Mol. Biol. 266*, 1016−1031.
5. Korndorfer, I., Steipe, B., Huber, R., Tomschy, A., and Jaenicke, R. (1995) *J. Mol. Biol. 246*, 511−521.
6. Ladenstein, R., and Antranikian, G. (1998) *Adv. Biochem. Eng. Biotechnol. 61*, 37−85.
7. Jaenicke, R., Schurig, H., Beaucamp, N., and Ostendorp, R. (1996) *Adv. Protein Chem. 48*, 181−269.
8. Jaenicke, R., and Bohm, G. (1998) *Curr. Opin. Struct.Biol. 8*, 738−748.
9. Jaenicke, R. (2000) *Proc. Natl. Acad. Sci. U.S.A. 97*, 2962−2964.
10. Hernandez, G., Jenney, F. E. J., Adams, M. W., and LeMaster, D. M. (2000) *Proc. Natl. Acad. Sci. U.S.A. 97*, 3166−3170.
11. Gershenson, A., Schauerte, J. A., Giver, L., and Arnold, F. H. (2000) *Biochemistry 39*, 4658−4665.
12. Fitter, J., and Heberle, J. (2000) *Biophys. J. 79*, 1629−1636.
13. Panasik, N., Brenchley, J. E., and Farber, G. K. (2000) *Biochim. Biophys. Acta 1543*, 189−201.
14. Vihinen, M., and Mäntsälä, P. (1989) *Crit. Rev. Biochem. Mol. Biol. 24*, 329−418.
15. Tomazic, S. J., and Klibanov, A. M. (1988) *J. Biol. Chem. 263*, 3092−3096.
16. Kay, L. E. (1998) *Nat. Struct. Biol. 5* (Suppl.), 513−517.
17. Fitter, J., Verclas, S. A., Lechner, R. E., Seelert, H., and Dencher, N. A. (1998) *FEBS Lett. 43*3, 321−325.
18. Karplus, M. (2000) *J. Phys. Chem. B 104*, 11−27.
19. Machius, M., Wiegand, G., and Huber, R. (1995) *J. Mol. Biol. 246*, 545−559.
20. Violet, M., and Meunier J.-C. (1989) *Biochem. J. 263*, 665−670.
21. Declerck, N., Machius, M., Chambert, R., Wiegand, G., Huber, R., and Gaillardin, C. (1997) *Protein Eng. 10*, 541−549.
22. Feller, G., d'Amico, D., and Gerday, C. (1999) *Biochemistry 38*, 4613−4619.
23. Schmidt, F. X. (1989) in *Protein Structure: A Practical Approach* (Creighton, T. E., Ed.) pp 261−297, IRL Press, Oxford.
24. Pace, C. N., and Scholtz, J. M. (1989) in *Protein Structure: A Practical Approach* (Creighton, T. E., Ed.) pp 299−321, IRL Press, Oxford.
25. Eftink, M. R. (1994) *Biophys. J. 66*, 482−501.
26. Bird, R., and Hopkins, R. H. (1954) *Biochem. J. 56*, 86−89.
27. Yoo, Y. J., Hong, J., and Hatch, R. T. (1987) *Biotechnol. Bioeng. 30*, 147−151.
28. Lechner, R. E., Melzer, R., and Fitter, J. (1996) *Physica B 226*, 86−91.
29. Ruffle, B., Ollivier, J., Longeville, S., and Lechner, R. E. (2000) *Nucl. Instrum. Methods Phys. Res., Sect. A 449*, 322−330.
30. Fitter, J. (2000) *J. Phys. IV (France) 10*, 265−270.
31. Becktel, W. J., and Schellman, J. A. (1987) *Biopolymers 26*, 1859−1877.
32. Suzuki, Y., Ito, N., Yuuki, T., Yamagata, H., and Udaka, S. (1989) *J. Biol. Chem. 264*, 18933−18938.
33. Yang, A. S., and Honig, B. (1993) *J. Mol. Biol. 231*, 459−474.
34. Privalov, P. L., and Khechinashvili, N. N. (1974) *J. Mol. Biol. 86*, 665−684.
35. Laderman, K. A., Davis, B. R., Krutzsch, H. C., Lewis, M. S., Griko, Y. V., Privalov, P. L., and Anfinsen, C. B. (1993) *J. Biol. Chem. 268*, 24394−24401.
36. Bee, M. (1988) *Quasi-elastic Neutron Scattering*, Adam & Hilger, Philadelphia, PA.
37. Fitter, J., Herrmann, R., Hauss, T., Lechner, R. E., and Dencher, N. A. (2001) *Physica B 301*, 1−7.
38. Declerck, N., Machius, M., Wiegand, G., Huber, R., and Gaillardin, C. (2000) *J. Mol. Biol. 301*, 1041−1057.
39. Brzozowski, A. M., Lawson, D. M., Turkenburg, J. P., Bisgaard-Frantzen, H., Svendsen, A., Borchert, T. V., Dauter, Z., Wilson, K. S., and Davies, G. J. (2000) *Biochemistry 39*, 9099−9107.
40. Nielsen, J. E., and Borchert, T. V. (2000) *Biochim. Biophys. Acta 1543*, 253−274.

41. Lumry, R., and Eyring, H. (1954) *J. Phys. Chem. 58*, 110−120.
42. Matthews, B. W., Nicholson, H., and Becktel, W. J. (1987) *Proc. Natl. Acad. Sci. U.S.A. 84*, 6663−6667.
43. Kuroki, R., Kawakita, S., Nakamura, H., and Yutani, K. (1992) *Proc. Natl. Acad. Sci. U.S.A. 89*, 6803−6807.
44. Seewald, M. J., Pichumani, K., Stowell, C., Tibbals, B. V., Regan, L., and Stone, M. J. (2000) *Protein Sci. 9*, 1177−1193.
45. Vihinen, M. (1987) *Protein Eng. 1*, 477−480.
46. Varley, P. G., and Pain, R. H. (1991) *J. Mol. Biol. 220*, 531−538.
47. Zavodszky, P., Kardos, J., Svingor, A., and Petsko, G. A. (1998) *Proc. Natl. Acad. Sci. U.S.A. 95*, 7406−7411.
48. Tang, K. E., and Dill, K. A. (1998) *J. Biomol. Struct. Dyn. 16*, 397−411.
49. Bismuto, E., Nucci, R., Rossi, M., and Irace, G. (1999) *Proteins 35*, 163−172.
50. Zaccai, G., Tehei, M., Scherbakova, I., Serdyuk, I., and Gerez, C., and Pfister, C. (2000) *J. Phys. IV (France) 10*, 283−287.
51. Nicholson, L. K., Yamazaki, T., Torchia, D. A., Grzesiek, S., Bax, A., Stahl, S. J., Kaufman, J. D., Wingfield, P. T., Lam, P. Y., and Jadhav, P. K. (1995) *Nat. Struct. Biol. 2*, 274−280.
52. Feher, V. A., and Cavanagh, J. (1999) *Nature 400*, 289−293.
53. Heberle, J., Fitter, J., Sass, H. J., and Buldt, G. (2000) *Biophys. Chem. 85*, 229−248.
54. Somero, G. N. (1975) *J. Exp. Zool. 194*, 175−188.

BI010808B